

# Adsorption/Desorption of Carbon Suboxide (C<sub>3</sub>O<sub>2</sub>) on Amorphous and Crystalline Ice Films Monitored by Infrared Spectroscopy

I. Couturier-Tamburelli, T. Chiavassa,\* and J. Pourcin

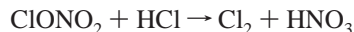
*Physique des Interactions Ioniques et Moléculaires, UMR 6633, Equipe de Spectrométries et Dynamique Moléculaire, Boîte 542, Université de Provence, F-13397 Marseille, Cedex 20, France*

*Received: August 25, 1998; In Final Form: December 9, 1998*

The carbon suboxide (C<sub>3</sub>O<sub>2</sub>) interactions with amorphous or crystalline ice surfaces in high vacuum are studied using temperature-programmed desorption (TPD) monitored by Fourier transform infrared spectroscopy (FTIR). We show clearly that unlike with crystalline film, in the 125–145 K temperature range, the adsorbate-covered amorphous ice surface presents a near monolayer state in which the C<sub>3</sub>O<sub>2</sub> forms a hydrogen bond with the free OH groups of the ice surface. The C<sub>3</sub>O<sub>2</sub> desorption from amorphous ice film seems to be induced by the onset of the crystallization of the amorphous ice into the cubic state. The activation energy for desorption is evaluated from a first-order regime to be  $43 \pm 2$  kJ mol<sup>-1</sup> and is consistent with the existence of a hydrogen-bonded adsorbed state.

## Introduction

Water ice, detected by infrared spectroscopy, is known to be present as a major component in comets, interstellar dusts,<sup>1–4</sup> or polar stratospheric clouds (PSCs).<sup>5–6</sup> For most of these systems, water ice is more often found to be amorphous than crystalline.<sup>7–8</sup> The physical properties of amorphous water ice (density, porosity, surface area, etc.) could explain its role as a catalyst in heterogeneous reactions occurring between impurities trapped at the ice surface. The two hydrochloration reactions indicated below<sup>9,10</sup> are typical examples of this kind of heterogeneous reaction:



Under laboratory conditions, the preparation of amorphous or crystalline water ice films from water vapor deposited on a cold window depends on the deposition conditions (temperature, pressure, rate). The characterization of these two types of ice can be easily realized using infrared spectroscopy.<sup>10–11</sup>

The aim of this work is to assess the chemical stability of carbon suboxide (C<sub>3</sub>O<sub>2</sub>), a molecule which is thought to be present in interstellar ices<sup>12</sup> and in the Halley comet nucleus,<sup>13</sup> adsorbed on water ice surfaces. We report and compare the results relative to the adsorption and desorption kinetics of C<sub>3</sub>O<sub>2</sub> on amorphous or crystalline ice thin films (0.1 μm thick) under low vacuum conditions ( $P = 10^{-5}$ – $10^{-6}$  mbar).

A particular adsorption state, in the 125–145 K temperature range, has only been detected for C<sub>3</sub>O<sub>2</sub> deposited on an amorphous water ice film. It appears that the C<sub>3</sub>O<sub>2</sub> desorption is induced by the water ice crystallization process. We were able to measure the desorption activation energy value for C<sub>3</sub>O<sub>2</sub> on an amorphous ice film by the temperature-programmed desorption (TPD) method monitored by FTIR spectroscopy for the first time. Results provide information on a possible

hydrogen bond interaction existing between C<sub>3</sub>O<sub>2</sub> and water molecules of the ice surface.

## Experimental Section

The C<sub>3</sub>O<sub>2</sub>, previously prepared as described by Long et al.,<sup>14</sup> is studied when it is adsorbed at 80 K on low-density amorphous (the most familiar form) or crystalline ice films, then linearly heated from 80 to 180 K (last temperature at which the ice film sublimates under our working pressure).

Low-density amorphous ice films are obtained from water vapor, deposited with approximately 1 nm s<sup>-1</sup> growth rate on a CsBr window held at 80 K under the constant and basic pressure of a cryostat ( $P = 10^{-5}$ – $10^{-6}$  mbar). Under these conditions, amorphous ice is microporous, leaving gaps within the ice bulk.<sup>15</sup>

Crystalline ice films are prepared using the following procedure: amorphous ice is deposited at 80 K then heated to 165 K during 1 h and cooled to 80 K again. Upon heating to this high temperature, the ice is transformed into the cubic crystalline structure, which is the predicted one.<sup>16–17</sup> However, according to Jenniskens et al.<sup>16,17</sup> the crystallization is not complete and an amorphous component is still intimately mixed with the cubic state into the crystallites.

The infrared transmission measurements, using a Nicolet 7199 FTIR spectrometer, are carried out on thin films of approximately 0.1 μm thickness in order to avoid the influence of the underlying window on the ice film properties. Film thicknesses cited above are approximately deduced from calibration of the infrared absorbance changes versus film thickness using optical interference.<sup>18</sup>

The spectra reported herein have been measured in the wavenumber range 400–4000 cm<sup>-1</sup> at 1 cm<sup>-1</sup> resolution. As the temperature was ramped with a β constant heating rate, interferograms were accumulated around a sample temperature (Ts) according to a maximum variation of 0.5 K corresponding to the chosen recording time.

We used a temperature-programmed desorption (TPD) method<sup>19,20</sup> to measure the activation energy for C<sub>3</sub>O<sub>2</sub> desorption

\* Author to whom all correspondence should be addressed.

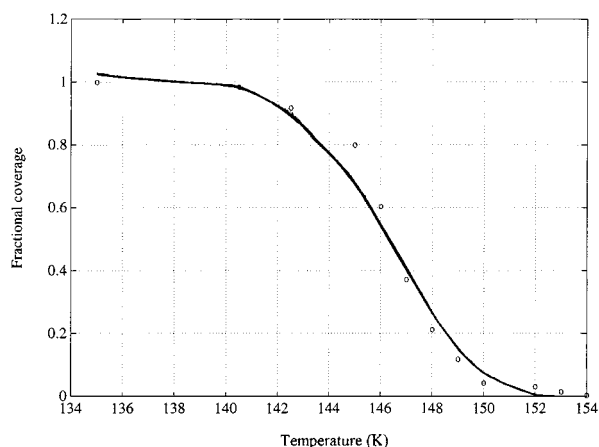


**Figure 1.** The desorption data in term of fractional coverage  $\theta$ , as defined in the text, are reported against the temperature  $T$  (K) and compared with the best fit by the model given in eq 1 for which,  $\beta = 5 \times 10^{-3} \text{ K s}^{-1}$ ,  $E_d = 43 \text{ kJ mol}^{-1}$ , and  $\nu_d = 10^{13} \text{ s}^{-1}$ . The monolayer at completion corresponds to a temperature  $T_0$  equal to 138 K. Points correspond to the experimental data and the line to the better fit obtained by the model given in eq 1.

from the water ice film in order to get information on the interaction strength between the adsorbate and the substrate. In our experimental procedure, the number of adsorbed species on the ice surface, at temperature  $T$  and gas pressure  $P$ , are evaluated from the integrated absorbance of the intense  $\nu_3$  vibrational mode ( $\text{C}=\text{O}$  antisymmetric stretching vibration) around  $2200 \text{ cm}^{-1}$ , of the adsorbed  $\text{C}_3\text{O}_2$ . Starting from the initial temperature  $T_0$ , for which  $N_0$  molecules of the adsorbate form a monolayer or a near monolayer state, the substrate has been linearly heated under the working pressure of the cryostat. From the spectral infrared absorbances, we define a fractional surface coverage,  $\theta$ , as the ratio of the average number  $N$  of adsorbed molecules at temperature  $T$  (at time  $t$ ) to  $N_0$ .

As an example we show in the Figure 1 the sublimation of a  $\text{C}_3\text{O}_2$  monolayer on an amorphous ice surface. These desorption data are analyzed in terms of a simple first-order model corresponding to the low coverage case:

$$\theta = \exp\left(\frac{-\nu_d(T - T_0)}{\beta}\right) \exp\left(\frac{-E_d}{RT}\right) \quad (1)$$

where  $\nu_d$  is the first-order preexponential term,  $E_d$  the activation energy for desorption, and  $R$  the gas constant.

The desorption rate at which the molecules leave the adsorption sites presents a maximum at the temperature  $T_{\text{max}}$  (the desorption peak temperature) for which the second derivative of  $\theta$  is zero. From eq 1, this zero value leads to the relation

$$\ln(\beta/RT_{\text{max}}^2) = -E_d/RT_{\text{max}} + \ln(E_d/\nu_d) \quad (2)$$

and the mean values of  $E_d$  and  $\nu_d$  can be determined from eq 2 by the linear regression of the data points in the heating rate range  $5 \times 10^{-3}$  to  $1.7 \times 10^{-2} \text{ K s}^{-1}$ .

## Results and Discussion

**A. Characterization of the Ice Films.** Under our experimental conditions, the ice film deposited at 80 K is considered as microporous and amorphous. Its infrared spectrum shown in Figure 2a is divided into three regions.

In the highest frequency range the bulk OH stretching modes of ice appear as a broad overlapped band, around  $3250 \text{ cm}^{-1}$ ,  $500 \text{ cm}^{-1}$  downshifted from the stretching modes of the free

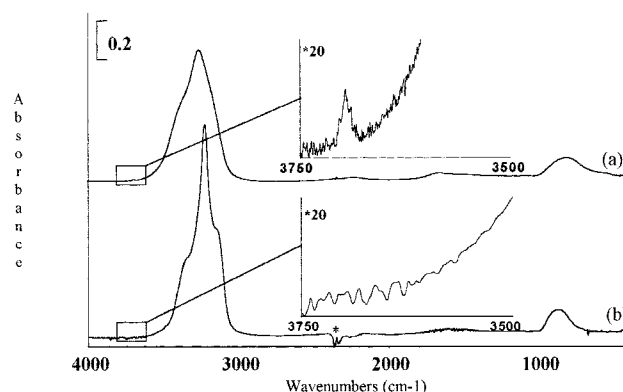


**Figure 2.** Infrared spectra of amorphous (a) and crystalline ice (b) at 80 K. The films are  $\approx 0.1 \mu\text{m}$  thick. The weak vibrational band denoted by an asterisk is attributed to gaseous  $\text{CO}_2$ . The insets showing the dangling mode at  $3695 \text{ cm}^{-1}$  in the amorphous ice (a) has completely disappeared after annealing at 160 K (b).

water molecules ( $\nu_{\text{OH}}$  symmetric =  $3657 \text{ cm}^{-1}$ ;  $\nu_{\text{OH}}$  antisymmetric =  $3756 \text{ cm}^{-1}$ ).

In the region near  $1600 \text{ cm}^{-1}$ , the band observed is assigned to the OH bending modes shifted from  $1595 \text{ cm}^{-1}$  in the gas phase to  $1640 \text{ cm}^{-1}$  in the bulk phase.

In the lowest frequency region of the spectrum, we observe at  $840 \text{ cm}^{-1}$  a vibrational band containing the hindered rotations of water molecules in the bulk, also known as librations.<sup>21</sup>

The most interesting spectral feature is the presence of the narrow ( $\approx 16 \text{ cm}^{-1}$  width) and weak peak at  $3695 \text{ cm}^{-1}$  which is known to be the stretching mode of OH groups in which the H atom is not involved in hydrogen bonding. This mode, also called “dangling”, is assigned to 3-coordinated water molecules existing both at the true surface of ice or at the surface of micropores within the ice bulk.<sup>22–23</sup> These dangling OH vibrational mode frequencies represent a good probe for testing the adsorption of impurities on amorphous ice surfaces.<sup>22–25</sup>

Figure 2b exhibits the infrared spectrum of crystalline thin film prepared following the annealing procedure described earlier. We clearly differentiate the amorphous and crystalline ices from their infrared spectra.<sup>11</sup> In particular, the crystalline ice presents the following unique characteristics: the bulk OH stretching modes appear as a well-resolved peak at  $3230 \text{ cm}^{-1}$  surrounded by two shoulders at  $3340$  and  $3150 \text{ cm}^{-1}$ . Note the narrowing of the bulk OH stretching modes in inset (b) in comparison with that of inset (a). Also a notable feature is the disappearance of the free OH stretch at  $3695 \text{ cm}^{-1}$  which is explained by a smaller density of dangling OH groups on the crystalline ice surface. This fact is correlated with an apparent reduction of the film surface area.

As observed by electron diffraction experiments<sup>16,17</sup> we are able in infrared spectroscopy to follow and characterize the change in structure of the low-density amorphous film prepared at 80 K and warmed from 80 to 180 K (temperature for which the ice layer sublimates at the working pressure). Upon heating ( $\beta = 8 \times 10^{-3} \text{ K s}^{-1}$ ) from 80 to 147 K, except for the reduction in intensity of the dangling mode due to a collapse of the pores,<sup>22</sup> no further spectral change is observed and the ice film persists in an amorphous form. By raising the temperature above 148 K the spectrum is irreversibly transformed to that characteristic of the crystalline film. The 148 K temperature indicates the onset of the amorphous ice crystallization into the cubic ice state and is related to the phase transition temperature. This temperature is found to be dependent on the heating rate. We found that for

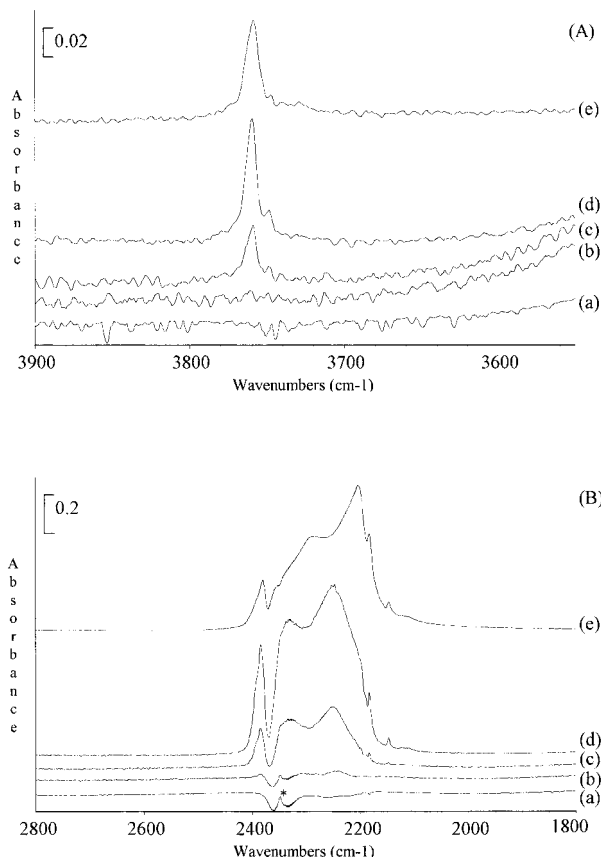


**Figure 3.** Selected infrared spectra resulting from a C<sub>3</sub>O<sub>2</sub> progressive exposure ( $10^{-6}$  mol s<sup>-1</sup>) on a crystalline ice film (thickness  $\approx 0.1$   $\mu$ m) maintained at 80 K, in the  $\nu_1 + \nu_4$  mode region (A) and in the  $\nu_3$  mode region (B) of C<sub>3</sub>O<sub>2</sub>. The weak vibrational band denoted by an asterisk is attributed to gaseous CO<sub>2</sub>. (a) Bare crystalline ice as reference, (b)  $10^{-5}$  mol, (c)  $3 \times 10^{-4}$  mol, (d)  $10^{-3}$  mol, (e) solid C<sub>3</sub>O<sub>2</sub> as reference.

a heating rate taken in the range  $5 \times 10^{-3}$  to  $1.7 \times 10^{-2}$  K s<sup>-1</sup>, the onset of cubic crystallization is observed in the 146–151 K range.

**B. Adsorption and Desorption of C<sub>3</sub>O<sub>2</sub> on Crystalline and Amorphous Ice Films.** The solid carbon suboxide infrared spectrum has been studied extensively in the past.<sup>26–27</sup> It is well-known that in a solid environment, C<sub>3</sub>O<sub>2</sub> adopts a bent form with a CCC bending angle close to 158°. Among all of the vibrational bands which can be observed, we consider two spectral regions around 2800–1800 and 3900–3600 cm<sup>-1</sup> which cover the intense  $\nu_3$  mode ( $\nu\text{C}=\text{O}_{\text{asym}}$ ) and the combination mode  $\nu_1 + \nu_4$  ( $\nu\text{C}=\text{O}_{\text{sym}} + \nu\text{C}=\text{C}_{\text{asym}}$ ).

Figure 3, parts A and B, in the 2800–1800 and 3900–3500 cm<sup>-1</sup> spectral ranges shows a representative set of infrared spectra resulting from the progressive C<sub>3</sub>O<sub>2</sub> exposure ( $\approx 10^{-6}$  mol s<sup>-1</sup>) of a crystalline ice film maintained at 80 K (spectra b–d). No change in the spectral line shape is observed with an increase of the C<sub>3</sub>O<sub>2</sub> exposure; the infrared spectrum is globally similar to that of the solid C<sub>3</sub>O<sub>2</sub> (spectrum e). During the temperature increase with a  $8 \times 10^{-3}$  K s<sup>-1</sup> heating rate, the C<sub>3</sub>O<sub>2</sub> deposited on crystalline ice sublimates at 120 K as for the pure solid C<sub>3</sub>O<sub>2</sub>. Thus an adsorption state corresponding to a C<sub>3</sub>O<sub>2</sub> monolayer on a crystalline ice surface seems not to be detectable, at least spectroscopically.

The C<sub>3</sub>O<sub>2</sub> adsorption on a bare amorphous ice film at 80 K (Figure 4, parts A and B, respectively, in the 2800–1800 and 3900–3500 cm<sup>-1</sup> spectral ranges) results in a downshift of 50 cm<sup>-1</sup> of the free OH stretching mode (Figure 4A). As with acetone or 2-propanol<sup>29</sup> this large shift indicates a selective

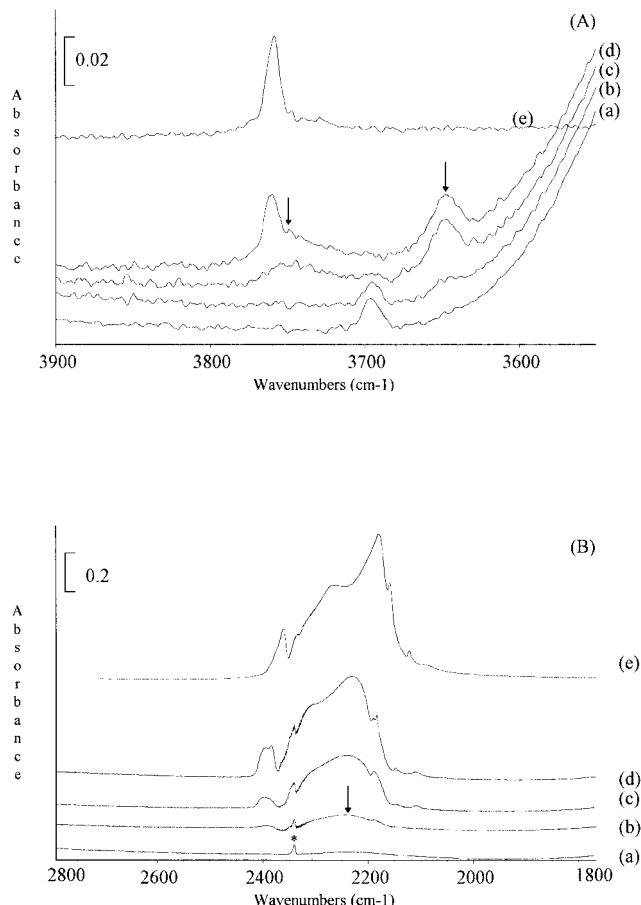


**Figure 4.** Selected infrared spectra resulting from a C<sub>3</sub>O<sub>2</sub> progressive exposure ( $10^{-6}$  mol s<sup>-1</sup>) on an amorphous ice film (thickness  $\approx 0.1$   $\mu$ m) maintained at 80 K, in the  $\nu_1 + \nu_4$  mode and in the dangling region (A) and in the  $\nu_3$  mode region (B) of C<sub>3</sub>O<sub>2</sub>. The weak vibrational band denoted by an asterisk is attributed to solid CO<sub>2</sub>, as impurity. C<sub>3</sub>O<sub>2</sub> associated directly with water molecules on the ice surface are shown by arrows. Note the 50 cm<sup>-1</sup> downshift of the dangling (Figure A, spectra a and c). (a) Bare crystalline ice as reference, (b)  $10^{-5}$  mol, (c)  $3 \times 10^{-4}$  mol, (d)  $10^{-3}$  mol, (e) solid C<sub>3</sub>O<sub>2</sub> as reference.

association of C<sub>3</sub>O<sub>2</sub> with the dangling OH bonds and takes into account the strong interaction between the adsorbate and the ice film. It supports our assumption of a hydrogen-bonded adsorbed state. This will be verified by the desorption activation energy measurement made in the following section.

The C<sub>3</sub>O<sub>2</sub> adsorption involves also the appearance of new weak vibrational bands centered at 3744 cm<sup>-1</sup> (Figure 4A, spectrum c) and 2241 cm<sup>-1</sup> (Figure 4B, spectrum c) resulting, respectively, from the  $\nu_1 + \nu_4$  and  $\nu_3$  modes of C<sub>3</sub>O<sub>2</sub> associated directly with water molecules on ice.

A further C<sub>3</sub>O<sub>2</sub> exposure involves the appearance of the same vibrational band shapes as those observed for the solid C<sub>3</sub>O<sub>2</sub> (Figure 4A, B, spectrum d) in comparison with Figure 4A, B, spectrum e). This should be correlated to a C<sub>3</sub>O<sub>2</sub> sticking on already-occupied adsorption sites.

In comparison with the crystalline case, pronounced differences are expected from the desorption process of C<sub>3</sub>O<sub>2</sub> on amorphous ice. Figure 5 shows selected infrared spectra recorded during the sample annealing from 80 K to the C<sub>3</sub>O<sub>2</sub> sublimation temperature with a heating rate of  $8 \times 10^{-3}$  K s<sup>-1</sup>. The desorption process can be followed in Figure 6 showing the  $\nu_3$  integrated band intensity variations as an estimation of the remaining C<sub>3</sub>O<sub>2</sub> molecules. Between 80 and 100 K (Figure 5a,b) the peak intensity is unchanged. At 120 K, we observe an abrupt decrease which results from the sublimation of solid C<sub>3</sub>O<sub>2</sub> as

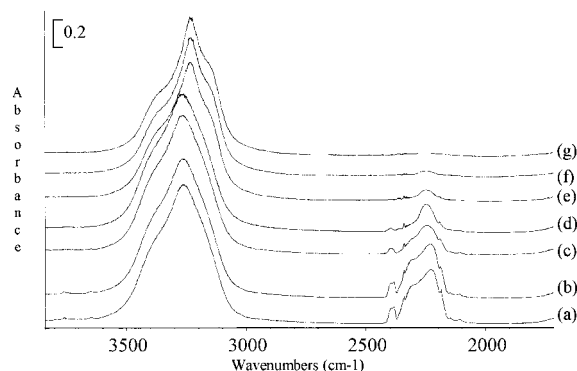


**Figure 5.** Selected infrared spectra during the temperature programmed desorption ( $\beta = 8 \times 10^{-3} \text{ K s}^{-1}$ ) of  $\text{C}_3\text{O}_2$  from amorphous ice surface, in the  $\nu_3$  mode region of  $\text{C}_3\text{O}_2$ . (a) 80 K, (b) 100 K, (c) 125 K, (d) 145 K, (e) 148 K, (f) 150 K, (g) 152 K.

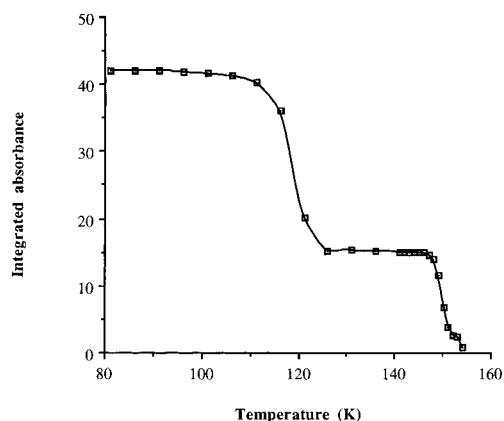


**Figure 6.** Integrated band intensities (in  $\text{cm}^{-1}$ ) in the  $2370\text{--}2150 \text{ cm}^{-1}$  range of the  $\text{C}_3\text{O}_2$   $\nu_3$  band, reported as a function of the temperature (K) following the results presented in Figure 5.

expected. From 125 to 145 K (Figure 5c,d, Figure 6), the amount of  $\text{C}_3\text{O}_2$  remains essentially constant. The spectral features of the  $\nu_3$  band (intensity, shape) are the same as those observed for  $\text{C}_3\text{O}_2$  interacting with amorphous ice (Figure 4A,B, spectrum b). Thus, this step confirms the existence of the adsorption state on amorphous ice previously described. In the 145–152 K range (Figure 5e–g, Figure 6), adsorbed  $\text{C}_3\text{O}_2$  starts to sublime. It is remarkable that this sublimation occurs at the beginning of the ice crystallization process, i.e., near the phase transition temperature at 148 K. This abrupt desorption probably occurs during the nucleation and growth of crystalline ice from amorphous water via a dynamic percolation mechanism already described by Kay and co-workers.<sup>30–31</sup> The kinetics of  $\text{C}_3\text{O}_2$  desorption from ice in the 135–155 K temperature range are well described by a first-order rate model. It allows an evaluation of the desorption activation energy using the temperature-programmed desorption (TPD) method as described in the Experimental Section.

**C. Activation Energy and Prefactor Measurements for  $\text{C}_3\text{O}_2$  Desorption.** The  $\text{C}_3\text{O}_2$  desorption kinetics from amorphous ice films of quasi constant thickness are studied in the first-order regime (low coverage case). Referring to Figure 6, we can link the step in the 125–145 K temperature range to the maximum capacity of a near monolayer state of  $\text{C}_3\text{O}_2$  adsorbed on an amorphous ice surface. In this temperature range, the fractional coverage,  $\theta$ , is taken equal to 1. We report in Table 1 experimental results obtained using four  $\beta$  values taken between  $5 \times 10^{-3}$  and  $1.7 \times 10^{-2} \text{ K s}^{-1}$ . One can clearly see the dependence of  $T_{\text{max}}$  on the  $\beta$  heating rate.

**TABLE 1. Desorption Peak Maximum Temperature ( $T_{\text{Max}}$ ) for Various  $\beta$  Heating Rates**

$\beta$ ( $\text{K s}^{-1}$ )	$T_{\text{max}}$ (K)
$5 \times 10^{-3}$	146.3
$8 \times 10^{-3}$	148.6
$1.3 \times 10^{-2}$	149.4
$1.7 \times 10^{-2}$	151.2

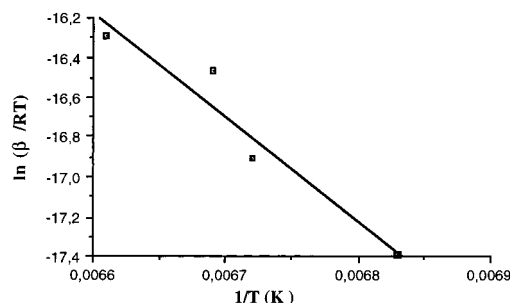


**Figure 7.** Desorption kinetics of  $\text{C}_3\text{O}_2$  from amorphous ice. The line is derived from a linear regression analysis of the data points.

$E_d$  and  $\nu_d$  were determined from a linear plotting of  $\ln(\beta/RT_{\text{max}}^2)$  vs  $1/T_{\text{max}}$  according to eq 2 (Figure 7). The data points fall on a straight line with relatively little scatter. From linear regression, we obtain  $E_d = 43 \pm 2 \text{ kJ mol}^{-1}$  and  $\nu_d$  about  $2 \times 10^{13} \text{ s}^{-1}$ . This prefactor lies quite enough within the range of values considered as acceptable for first-order desorption processes.<sup>19</sup> The  $E_d$  measured value is consistent with a process involving scission of a hydrogen bond between  $\text{C}_3\text{O}_2$  and a free OH as previously assumed. However, this value is also close to the activation enthalpy ( $44 \text{ kJ mol}^{-1}$ ) of the ice crystallization process.<sup>32</sup> We therefore think that  $\text{C}_3\text{O}_2$  desorption is induced by the reduction of the number of free hydroxyl adsorption sites and by the formation of new hydrogen bonds between water molecules during the ice crystallization.

## Conclusion

Physical–chemical properties of amorphous ice appear qualitatively different from those of a crystalline ice. On a crystalline film, no adsorption state is detected and the  $\text{C}_3\text{O}_2$  desorption temperature from the ice surface is analogous to the solid  $\text{C}_3\text{O}_2$  desorption temperature. Pronounced differences appear when  $\text{C}_3\text{O}_2$  is deposited on amorphous ice film. Such an ice implies by its microporosity a higher density of surface free OH groups with which the  $\text{C}_3\text{O}_2$  molecules are able to interact. The desorption activation energy measured ( $E_d \approx 43 \pm 2 \text{ kJ mol}^{-1}$ ) gives evidence of a hydrogen-bonded adsorbed state on amorphous films. It appears that the  $\text{C}_3\text{O}_2$  desorption process is probably induced by the onset of the ice crystallization from the amorphous ice film.

## References and Notes

- (1) Blake, D.; Allamandola, L.; Sanford, S.A.; Hudgins, D.; Freund, F. *Science* **1991**, 254, 548.
- (2) Mayer, E.; Pletzer, R. *Nature* **1986**, 319, 298.
- (3) Sanford, S.A.; Allamandola, L. *Icarus* **1988**, 76, 201.
- (4) Westly, M. S.; Baragiola, R. A.; Johnson, R. E.; Baratta, G. A. *Nature* **1995**, 373, 405.
- (5) Crutzen, P. J.; Arnold, F. *Nature* **1986**, 324, 651.
- (6) McElroy, M. B.; Salawitch, R. J.; Wofsy, S. C.; Logan, J. A. *Nature* **1986**, 321, 759.
- (7) Smith, R. G.; Sellgren, K.; Toganuga, A. T. *Astrophys. J.* **1988**, 334, 209.
- (8) Rouan, D.; Omont, A.; Lacombe, F.; Forveille, T. *Astron. Astrophys.* **1988**, 189, L3.
- (9) Solomon, S. *Rev. Geophys.* **1988**, 26, 131.

- (10) (a) Tamburelli, I.; Chiavassa, T.; Borget, F.; Pourcin, J. *J. Phys. Chem. A* **1998**, *102*, 423. (b) Couturier-Tamburelli, I. Thesis, Université de Provence, 1998.
- (11) Graham, J. D.; Roberts, J. T. *Geophys. Res. Lett.* **1995**, *22*, 251.
- (12) Strazzula, G.; Brucato, J. R.; Palumbo, M. E.; SaTorre, M. A. *Astron. Astrophys.* **1997**, *321*, 618.
- (13) Huntress, W. T.; Allen, M.; Delitsky, M. *Nature* **1991**, *352*, 316.
- (14) Long, D. A.; Murfin, F. S.; Williams, R. L. *Proc. R. Soc. London* **1954**, A 223, 251.
- (15) Mayer, E.; Pletzer, R. *Nature* **1986**, *319*, 298.
- (16) Jenniskens, P.; Blake, D. F. *Science* **1994**, *265*, 753.
- (17) Jenniskens, P.; Banham, S. F.; Blake, D. F.; McCoustra, M. R. S. *J. Chem. Phys.* **1997**, *107*, 1232.
- (18) Zondlo, M. A.; Onasch, T. B.; Warshavsky, M. S.; Tolbert, M. A.; Mallich, G.; Arentz, P.; Robinson, M. S. *J. Phys. Chem B* **1997**, *101*, 10887.
- (19) Yates, J. T. *Methods Exp. Phys.* **1985**, *22*, 425.
- (20) Readhead, P. A. *Vacuum* **1962**, *12*, 203.
- (21) Callen, B. W.; Griffiths, K.; Norton, P. R. *Surf. Sci. Lett.* **1992**, *261*, 44.
- (22) Rowland, B.; Devlin, J. P. *J. Chem. Phys.* **1991**, *94*, 812.
- (23) Buch, V.; Devlin, J. P. *J. Chem. Phys.* **1991**, *94*, 4091.
- (24) Schaff, J. E.; Roberts, J. T. *J. Phys. Chem.* **1996**, *100*, 14151.
- (25) Givan, A.; Loewenschuss, A.; Nielsen, C. J. *Vib. Spectrosc.* **1996**, *12*, 1.
- (26) Miller, F. A.; Fateley, W. G. *Spectrochim. Acta* **1964**, *20*, 253.
- (27) Smith, W. H.; Leroi, G. E. *J. Chem. Phys.* **1966**, *45*, 1767.
- (28) Pietri, N.; Tamburelli, I.; Aycard, J. P.; Chiavassa, T. *J. Mol. Struct.* **1997**, *416*, 187.
- (29) Schaff, J. E.; Roberts, J. T. *J. Phys. Chem.* **1996**, *100*, 14151.
- (30) Smith, R. S.; Huang, C.; Wong, E. K. L.; Kay, B. D. *Phys. Rev. Lett.* **1997**, *79*, 909.
- (31) Smith, R. S.; Huang, C.; Wong, E. K. L.; Kay, B. D. *Surf. Sci.* **1996**, *367*, 13.
- (32) Schmitt, B.; Grim, R.; Greenberg, M. In 22nd Eslab Symposium on Infrared Spectroscopy in Astronomy (ESA-SP 290), Salamanca, Spain, 1989; p 213.